Roles of Cu codoping and oxygen vacancies on ferromagnetism in In_2O_3:Fe

L. X. Guan, J. G. Tao, Z. R. Xiao, B. C. Zhao, X. F. Fan, C. H. A. Huan, J. L. Kuo,* and L. Wang†
Division of Physics and Applied Physics, School of Physical and Mathematical Sciences, Nanyang Technological University, Singapore 637371, Singapore

(Received 10 February 2009; revised manuscript received 7 April 2009; published 11 May 2009)

The electronic structures and the ferromagnetic (FM) stability in In_2O_3:Fe (IFO) with additional Cu and oxygen vacancy (V_O) doping have been investigated using first-principles calculations within the framework of density-functional theory. It is found that pure IFO has an antiferromagnetic ground state, but the existence of V_O or with Cu codoping could lead to a weak FM coupling in IFO system for some special configurations. The stability of the ferromagnetism is greatly enhanced by the coexistence of V_O and Cu codoping in IFO system. We demonstrate that the role of Cu ions is to act as superexchange mediators causing an indirect FM coupling between Fe cations through the hybridization of the Cu $3d$ states with the O $2p$ states. The delocalized hybridization consisted of Fe $3d$, O $2p$, and Cu $3d$ is found to be very efficient to mediate the FM exchange interaction. In favor of the FM state, Cu ions prefer to locate adjacent to the Fe ions in order to form Fe1-O1-Cu-O2-Fe2 coupling chain. The results of our calculations suggest the possibility of fabricating In_2O_3 based transparent spintronics by (Fe, Cu) codoping in a reduced growth ambient.

DOI: 10.1103/PhysRevB.79.184412 PACS number(s): 75.50.Pp, 75.30.Hx, 71.20.−b, 75.30.Et

I. INTRODUCTION

The prediction of room-temperature (RT) ferromagnetism in Mn-doped ZnO and GaN by Dietl *et al.*[1] has triggered extensive studies on oxide-based diluted magnetic semiconductors (DMSs).[2–11] In_2O_3 being one of the candidate hosts is a technologically important transparent semiconductor with a direct band gap of 3.75 eV.[12] In form of thin films, In_2O_3 is superior to other transparent conductors because of the high mobility ($10-75$ cm^2 V^{-1} s^{-1}) with a carrier density of $\sim 10^{19}-10^{20}$ e cm^{-3}.[13] RT ferromagnetism can be achieved[9–11,14,15] by doping or codoping of $3d$ transition-metal (TM) impurities into In_2O_3, which is attractive due to its integration of optical, electronic, and magnetic properties into one single material. Codoping has attracted attention primarily due to the possibility to tailor the position and occupancy of the Fermi level (E_F) of the doped DMS.[16–20]

Recently, there are abundant yet controversial experimental reports on $3d$ TMs-doped In_2O_3. The magnetic states of $3d$ TMs-doped In_2O_3 are determined by several factors such as the synthesis methods, the existence of oxygen vacancies (V_O), or codoping. It was reported that In_2O_3 doped with V,[3] Cr,[9,21] Fe,[14,15] Co,[22] and Ni (Refs. 23 and 24) exhibit strong RT ferromagnetism. On the contrary, Mn-, V-, Fe-, or Cu-doped In_2O_3 have been found to show no evidence of ferromagnetism.[25–27] Numerous experimental findings as well as some previous first-principles calculations of the electronic structure and magnetic interaction of the doped, especially TMs-doped oxide-based DMS,[4,14,15,21,28–30] suggest that the vacancies or some other defects induced during the sample preparation process may serve as important factors to introduce ferromagnetism in these kinds of materials. Among all TMs-doped In_2O_3, Fe-doped In_2O_3 (In_2O_3:Fe, IFO) is a suitable prototype system for study due to the high solubility of Fe in the In_2O_3 (>20%) and a homogeneous solid solution can be realized at least up to 15% Fe doping.[14,30] Cu has been codoped with Fe into In_2O_3 (IFCO) in order to achieve multiple oxidation states of Fe^{2+} and Fe^{3+}, which has been reported to be essential for exhibiting ferromagnetic (FM) coupling.[14,15,30,31] To the best of our knowledge, up to now, there are very few theoretical studies on the origin of ferromagnetism in TMs-doped In_2O_3, especially TMs-codoped In_2O_3. All these make theoretical investigation highly desirable for solving the puzzle and exploring the origin of the ferromagnetism in TMs-doped In_2O_3.

In the present work, we performed a systematical study for the evolution of the ferromagnetism in IFO system while involving Cu codoping as well as V_O into the system. We report the results of detail first-principles calculations on the electronic structure and magnetic properties of the IFCO system and demonstrate the key roles of the Cu codoping and V_O in the developing of ferromagnetism in this system. This paper is organized as follows. Section II presents computational details of the first-principles calculations. Section III discusses the results in terms of V_O effect, Cu codoping effect, as well as V_O and Cu coexistence effect on the ferromagnetism in the IFO system. In Sec. IV, we present our conclusions on this work.

II. THEORETICAL METHOD

Our calculations are carried out with a periodic supercell model within the framework of density-functional theory (DFT) using the full potential projector augmented plane-wave (PAW) (Ref. 32) method with a plane-wave basis set, as implemented in the Vienna *ab initio* Simulation Package (VASP).[33–35] The energy cutoff is set to 500 eV for the plane-wave basis, and the exchange-correlation functional is treated by Perdew-Burke-Ernzerhof form generalized gradient approximation (GGA-PBE).[36] The Gaussian smearing method with a smearing parameter of 0.1 eV is used for all calculations due to the weak metallicity induced by doping. For all doping configurations, both the spin polarized and non-spin-polarized calculations were performed and the symmetry unrestricted structure optimizations are carried out using a conjugate gradient algorithm with a force conver-

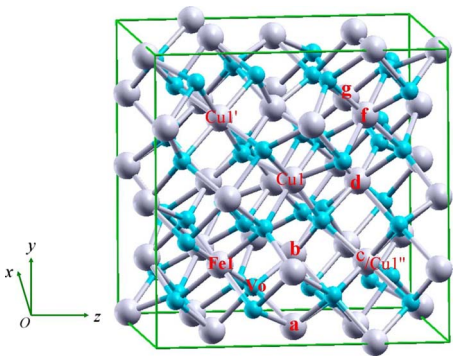

FIG. 1. (Color online) Crystal structure of In_2O_3. Gray (big) and cyan (small) spheres are In and O atoms. For IFO systems we examined, one of the two Fe atoms is fixed at the position labeled Fe1, and the other one (Fe2) locates at the positions labeled with *a*, *b*, *c*, *d*, *f*, and *g* in different configurations. For IFCO-V_O systems, the positions of the Cu dopant are labeled with Cu1, Cu1′, and Cu1″ for different configurations. The position of oxygen vacancy is labeled with V_O for all IFO-V_O configurations.

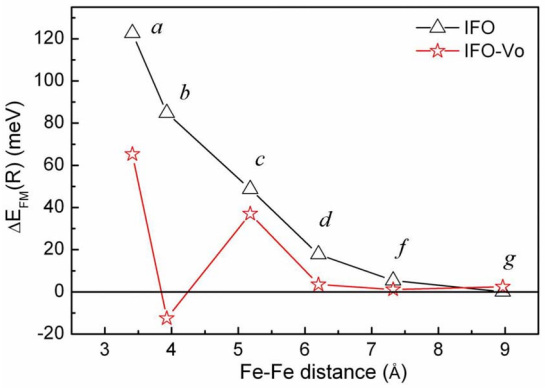

FIG. 2. (Color online) The evolution of ferromagnetic stabilization energy (ΔE_{FM}) as a function of the Fe-Fe separation distance in IFO and IFO-V_O systems. The letters next to data indicate the configurations (see text).

gence criterion of 2×10^{-2} eV/Å. The Brillouin zone was sampled by $3\times3\times3$ Monkhorst-Pack *k*-point grids for geometry optimizations and then sampled by the finer $4\times4\times4$ grids for the self-consistent energy calculations. For density of states (DOS) spectrum calculations, self-consistent field (SCF) energy is converged to 10^{-6} eV.

The selected supercell is composed of 80 atoms, corresponding to 16 f.u. In_2O_3. The supercell size is large enough to allow us to investigate various configurations of Fe doping and Fe, Cu codoping, as well as to isolate the interaction between impurities in some configurations. According to the Wyckoff's notation, there are eight In(1) atoms occupying the *b* sites, 24 In(2) atoms occupying the *d* sites, and 48 oxygen atoms occupying the *e* sites in such a supercell. In our calculations, first, two In atoms were substituted by two Fe dopants. We fixed one dopant Fe atom (denoted by Fe1) at In(1) position because it was reported to be the favorable position for dopant.[37] In the present work, we vary the possible positions of the second dopant Fe atom (denoted by Fe2) within the fourth nearest-neighbor (NN) to Fe1, face-diagonal position, and body-diagonal position with respect to Fe1 in the sublattice of the cubic In(1). These configurations are defined as *a*, *b*, *c*, *d*, *f*, and *g*, for first NN, second NN, third NN, fourth NN, face-diagonal, and body-diagonal positions, respectively, as shown in Fig. 1. Each configuration is further doped with an additional Cu atom. The variation of Cu position is also considered as a function of the separation distance to the two Fe atoms. In the present work, the studied positions of this additional Cu atom are labeled as Cu1, Cu1′, and Cu1″ in Fig. 1, respectively. In the following, we use *i*, *ii*, and *iii* as short-hand notation to represent Cu1, Cu1′, and Cu1″, respectively. Moreover an oxygen vacancy (V_O) is introduced by removing one oxygen atom adjacent to Fe or Cu or neither; the configurations with V_O in vicinity of Fe1 are denoted as V_O in Fig. 1. All these dopant configurations are represented by a label, such as *b*-IFCO-V_O-*i*, where *b* represents the configurations of the two Fe atoms, IFCO means the system is Fe and Cu codoped In_2O_3 system, V_O indicates the existence of oxygen vacancy, and *i* represents the Cu1 position for the doped Cu atom. For all dopant configurations, the FM stabilization energy $\Delta E_{FM}(R)=E_{FM}(R)-E_{AFM}(R)$ is calculated, where $E_{FM}(R)$ and $E_{AFM}(R)$ are the total energies of the supercell with FM and antiferromagnetic (AFM) aligned Fe pairs, respectively, with the Fe-Fe separation distance of *R*. The difference in the two energies yields the *J* coupling, indicating relative stability of the AFM and FM states.

III. RESULTS AND DISCUSSIONS

A. Oxygen vacancy (V_O) effect

At first, we discuss the role that V_O plays in the IFO system. Figure 2 presents the variation of FM stabilization energies (ΔE_{FM}) as a function of Fe-Fe separation distance both with and without V_O. In the absence of V_O, AFM spin ordering predominates over the exchange interaction for all studied configurations. Decrease in the magnitude of ΔE_{FM} as Fe-Fe distance increases suggests that AFM superexchange between the dopants is intermediated via the bridging oxygen (O_{br}) ions.[4] It turns to saturate and approaches zero when the separation of Fe-Fe reaches around 7.5 Å. The fade out of AFM coupling may be due to the screening by the free carriers in the system.[37] Our results are consistent with the work done on V-doped In_2O_3,[3] where the FM and AFM states are degenerate when the doped V pairs are separated by 8.76 Å.

As shown in Fig. 2, after introducing V_O into the IFO system, the AFM spin ordering still prevails but the coupling is softened with the presence of V_O. The dramatic change of the favorable magnetic ordering in *b*-IFO-V_O is very surprising, where the ΔE_{FM} is a negative value, implying an energetic FM favorable ground state. In *b*-IFO-V_O configuration, the only existing O_{br} between the Fe1 and Fe2 has been removed by the way we introduce the V_O as stated in the preceding section. These results provide strong evidence that the role of O_{br} is to mediate the superexchange interaction for AFM coupling. The dual spin-density distribution around the O_{br}, as shown in Fig. 3, confirms the nature of O_{br} serv-

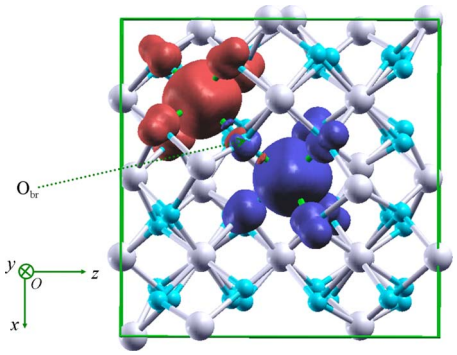

FIG. 3. (Color online) Spatial spin-density distribution of *b*-IFO configuration in AFM ordering. Red and blue isosurfaces correspond to spin-up and spin-down regions.

ing as a bridge for the AFM interactions between dopant Fe atoms. The main calculation results of IFO and IFO-V_O systems are tabulated in Table I.

Electrons induced by introducing V_O result in mixed valence of Fe^{2+} and Fe^{3+} ions, as supported by the reduced projected magnetic moments of Fe, which are $3.95\mu_B$/Fe and $3.77\mu_B$/Fe in *b*-IFO and *b*-IFO-V_O systems, respectively, as shown in Table I. This corroborates the previous findings of the connection between the presence of Fe^{2+} and FM coupling,[10] which sustains that the FM coupling is mediated by delocalized carriers. Nevertheless, even for *b*-IFO-V_O configuration, the FM coupling is weak (ΔE_{FM} =−12.5 meV).

Figure 4 gives the DOS spectra of *b*-IFO and *b*-IFO-V_O in FM ordering. The Fe *d* states are more sensitive to the surrounding oxygen than the spherically symmetric *s* states of In atoms. As shown in Fig. 4(c), for IFO system, Fe 3*d* electrons are mainly distributed in the valence band due to the hybridization with the O 2*p* states, leaving the unoccupied minority states in the conduction band. However, the Fermi level (E_F) is located in the impurity states rather than the conduction band. After introducing V_O, as shown in Fig. 4(b), the position of E_F is slightly raised to the conduction-band minimum. The Fe 3*d* minority states, as displayed in Fig. 4(d), are partially occupied leading to the mixed valance of Fe^{2+} and Fe^{3+}, which can drive ferromagnetism.[11] The electronic states in the gap are due to the hybridization between *d* states of Fe and *p* bands of oxygen, which mediates the magnetic interactions.[8]

The total-energy minimum calculations for all the dopants configurations indicate that the *b*-IFO and *b*-IFO-V_O are the most energetically favorable structures. In favor of *b* configuration, the doped Fe atoms are intended to accumulate together with a short Fe-Fe distance of ~3.9 Å. Generally speaking, the shorter Fe-Fe distance implies a larger doping concentration. This interpretation has been supported by our recent experimental finding[30] as well as some other reports[14,15] that the FM coupling appears only when the Fe concentration is higher than a critical value (10% in Ref. 15), while paramagnetic (PM) state is more stable with lower Fe dose.

B. Cu codoping effect: Short-range weak indirect FM coupling mediator

In this section, we discuss the Cu codoping effect for the IFO system. The additional doping of Cu into *b*-IFO renders the system, *b*-IFCO-*i*, a weak FM ground state with ΔE_{FM} of

TABLE I. The calculation results of IFO system with and without oxygen vacancy (V_O). The FM stabilization energies (ΔE_{FM}) and the total (M_{total}) and projected magnetic moments for Fe (M_{Fe}) in both FM and AFM orderings are summarized.

		M_{total} (μ_B)		M_{Fe} (μ_B)			
				FM		AFM	
Notation	ΔE_{FM} (meV)	FM	AFM	Fe1	Fe2	Fe1	Fe2
			Only Fe impurities				
a-IFO	122.7	9.94	0.00	3.95	3.94	3.91	−3.89
b-IFO	84.8	9.82	0.03	3.97	3.91	3.95	−3.90
c-IFO	48.7	9.98	0.00	3.99	3.97	3.98	−3.96
d-IFO	17.8	9.93	0.04	3.99	3.94	3.97	−3.93
f-IFO	5.4	9.96	0.00	3.98	3.98	3.98	−3.98
g-IFO	0.03	9.96	0.00	3.98	3.98	3.98	−3.98
			With oxygen vacancy				
a-IFO-V_O	65.3	9.03	0.13	3.79	3.77	3.75	−3.69
b-IFO-V_O	−12.5	9.13	0.02	3.77	3.77	3.76	−3.77
c-IFO-V_O	37.0	9.41	−0.01	3.81	3.90	3.80	−3.88
d-IFO-V_O	3.5	9.41	−0.32	3.76	3.94	3.76	−3.95
f-IFO-V_O	1.1	9.43	0.23	3.95	3.79	3.95	−3.79
g-IFO-V_O	2.4	9.45	−0.29	3.78	3.96	3.78	−3.96

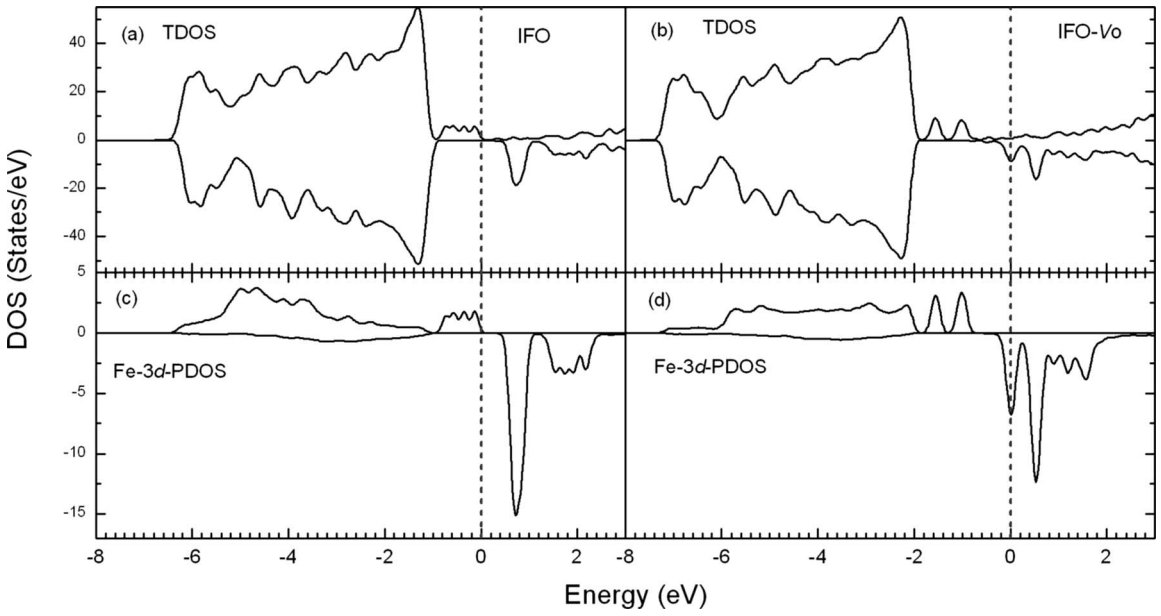

FIG. 4. The total DOSs (TDOSs) of (a) *b*-IFO and (b) *b*-IFO-V_O and Fe 3*d* PDOSs of (c) *b*-IFO and (d) *b*-IFO-V_O in FM ordering. The vertical line drawn indicates the E_F position. The spin-up and spin-down DOSs are shown above and below the abscissa axis.

−7.3 meV. This result accords with the prediction that Cu doping was found not to be directly responsible for the RT ferromagnetism of IFCO system.[10,14] After introducing Fe and Cu ions into In_2O_3, significant local structure distortions occur at the Fe- and Cu-substitution sites. The optimized Fe-O bond lengths are about ~14% smaller in comparison to that of In-O in the optimized pure In_2O_3. The shorter Fe-O distance may be due to the reduction of oxygen-oxygen repulsion forces[10] and coincides with the fact that the radii of both Fe^{3+} and Fe^{2+} are smaller than that of In^{3+}. The change of the six Cu-O bond lengths, which form the Cu-O octahedral, is rather complicated. Two of them are shortened by ~7%, the other two are increased by ~7%, while the last two remain the same length as compared to that of In-O in the optimized pure In_2O_3. The local distortions change the lattice structure to one with a lower symmetry, resulting in a nearly complete splitting of the 3*d* orbitals. In Fig. 5(a), the E_F crosses the majority spin of impurity levels. One main feature indicated in the DOS spectra is the *d* hole states located at the top of the impurity band in the gap. As shown in Figs. 5(b)–5(d), there are strong *d*-*p*-*d* hybridizations between Cu, O_{br}, and Fe, which induce localized distributed holes in Fe 3*d* states. The localized *d* holes are also present in those configurations with V_O where FM ordering is stable (such as *b*-IFCO-V_O-*i*) but disappear in configurations where AFM ordering is stable (such as *b*-IFCO-V_O-*ii*). (We will discuss this further in next section.) All these findings strongly suggest that the localized spatial distributed *d* holes of Fe atoms induced by additional Cu doping play a vital role for the indirect FM exchange interaction between Fe1 and Fe2 atoms via Cu mediator. The existence of the hole states agrees with the lower oxidation state of Cu than Fe and In, which can be deduced from the projected magnetic moment (~-0.4μ_B).

The role of Cu is found to enhance the stability of ferromagnetism between the dopant Fe atoms, analogical to that in Cu- and Co-codoped ZnO.[20] The spin-density distributions, as shown in Fig. 6, corroborate the existence of the Cu-mediated FM interaction in IFCO system. The Cu ion being spin polarized by the presence of the magnetic impurities shown in Fig. 6 mediated an indirect magnetic interaction among them.[20] However, the Cu-mediated interaction is highly anisotropic as evidenced by the spin density shown in Fig. 6. This can be attributed to the band filling of the *d* orbitals of Cu and their directionality. Furthermore, a coupling chain of Fe1-O1-Cu-O2-Fe2 can be easily recognized in Fig. 6.

C. Cu and V_O codoping effect: The role to RT ferromagnetism

As discussed above, V_O or Cu doping alone in IFO system can improve the FM coupling but neither of them is sufficient enough to achieve stable RT ferromagnetism. We thus consider a system involving both V_O and Cu codopings. This is also motivated by the experiment finding that the IFCO system shows ferromagnetism when the samples are prepared under low oxygen pressure.[15] Our main calculation results of IFCO and IFCO-V_O are summarized in Table II involving the ferromagnetic stabilization energy and magnetic moments of Fe and Cu for each configuration studied. As can be seen in Table II, by introducing of V_O into *b*-IFCO-*i* system (*b* configuration has been demonstrated to be more energetically stable), a pronounced enhancement of the stability of the FM state was found (ΔE_{FM}= −90.4 meV).

To investigate the mechanism of the FM coupling, we first inspect the electronic structure of *b*-IFCO-V_O-*i*. Figures 5(e)–5(h) present the DOS spectra of *b*-IFCO-V_O-*i* in FM ordering. As displayed in Figs. 5(f)–5(h), Fe 3*d*, Cu 3*d*, and 2*p* states of O_{br} all span the same energy space, i.e., from the bottom of the valance band to E_F, which indicates that there exists a strong hybridization between *d* orbital of TMs (Fe

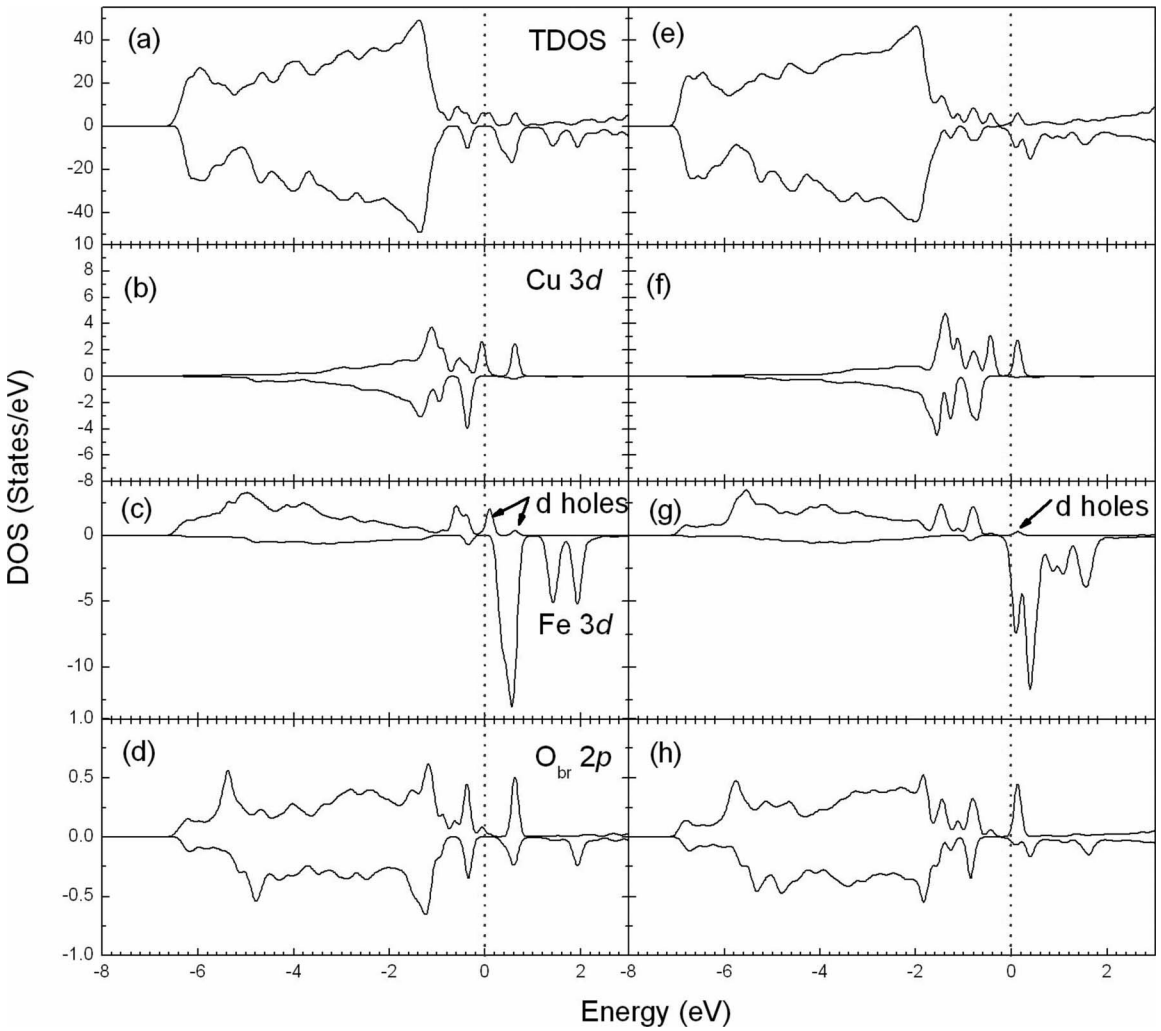

FIG. 5. The TDOSs and PDOSs of Cu 3*d*, Fe 3*d*, and O_{br} 2*p* for [(a)–(d)] *b*-IFCO-*i* and [(e)–(h)] *b*-IFCO-V_O-*i* in FM ordering, respectively. The vertical line drawn indicates the E_F position. The spin-up and spin-down DOSs are shown above and below the abscissa axis.

and Cu) and *p* orbital of intermediate oxygen atoms inside the host lattice. The hybridization between the TMs and their surrounding oxygen atoms also induced significant net magnetic moments on these oxygen atoms. Therefore, the total magnetic moments are mainly derived from the complex consisting of the dopants and the neighboring O anions in these systems. Moreover, the introduction of V_O results in more electrons compensating the holes in the majority-spin states in Fe *d* bands induced by Cu doping. However, there still presents a small amount *d* holes in the conduction band of the majority-spin states. For *b*-IFCO-V_O-*ii* configuration, which is stable in AFM ordering, the *d* holes in the majority-spin states are totally compensated. Combining the *d* hole feature and the magnetic ordering state of these two configurations, it is obvious that the holes in the Fe *d* bands generated by the Cu codoping play an important role in the FM exchange coupling in IFCO-V_O system. The increased FM coupling for V_O-doped IFCO confirms the essential role of the electrons induced by V_O, together with holes induced by Cu codoping, in mediating the FM interaction.

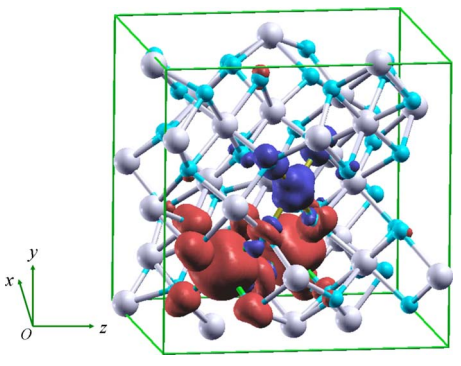

FIG. 6. (Color online) Spatial spin-density distribution of *b*-IFCO-*i* configuration in FM ordering. Red and blue isosurfaces correspond to spin-up and spin-down regions.

The strong AFM interaction between the *d* orbitals of both the two Fe atoms and Cu is mediated by *p* orbital of the O_{br} atoms, which brings on a strong indirect FM coupling between Fe1 and Fe2 atoms. The indirect FM coupling is very strong with the ΔE_{FM} in the magnitude of −90.4 meV (for *b*-IFCO-V_O-*i* configuration), which agrees with the reports by Lathiotakis *et al.*[20] and Ye *et al.*[38] To further investigate

TABLE II. FM stabilization energies (ΔE_{FM}) of IFCO and IFCO-V_O systems. The total (M_{total}) and the projected magnetic moments for Fe (M_{Fe}) and Cu (M_{Cu}) in both FM and AFM orderings are also summarized.

		M_{total} (μ_B)		M_{Fe} (μ_B)				M_{Cu} (μ_B)	
				FM		AFM			
Notation	ΔE_{FM} (meV)	FM	AFM	Fe1	Fe2	Fe1	Fe2	FM	AFM
Only Fe and Cu impurities									
b-IFCO-*i*	−7.3	7.97	0.02	3.55	3.52	3.34	−3.55	−0.37	−0.21
c-IFCO-*i*	−9.4	7.97	0.00	3.53	3.53	3.51	−3.51	−0.37	0.00
With oxygen vacancy									
b-IFCO-V_O-*i*	−90.4	8.66	−0.12	3.71	3.73	3.70	−3.71	−0.37	−0.06
b-IFCO-V_O-*ii*	7.1	9.00	−0.70	3.85	3.86	3.85	−3.85	−0.48	−0.48
b-IFCO-V_O-*iii*	−45.6	8.97	0.16	3.84	3.74	3.84	−3.66	−0.41	−0.06
c-IFCO-V_O-*i*	−110.5	8.24	0.60	3.72	3.69	3.57	−3.34	−0.38	0.01
f-IFCO-V_O-*i*	−35.6	8.95	−0.67	3.83	3.77	3.81	−3.84	−0.33	−0.33

the correlation between the FM coupling and the strength of Fe1-O1-Cu-O2-Fe2 coupling chains, we vary the Fe2 position by remaining the Fe1, Cu, and V_O locations. The Fe2 is moved from Fe1's second NN to the third and the sixth NNs, corresponding to *c*-IFCO-V_O-*i* and *f*-IFCO-V_O-*i* configurations, respectively. In all these cases, the Fe1-O1-Cu-O2-Fe2 chains still exist. The ΔE_{FM} are found to be −110.5 and −35.6 meV for *c*- and *f*-IFCO-V_O-*i* configurations, respectively. The strongest FM coupling shown in *c*-IFCO-V_O-*i* configuration is due to the highest symmetry of this configuration compared to the other ones.[20] The dramatic reduction of ΔE_{FM} in *f*-IFCO-V_O-*i* configuration suggests a strong correlation between the FM coupling and the Fe-Fe distance in the Fe1-O1-Cu-O2-Fe2 coupling chains.

The effect of Cu positions with respect to Fe pairs is also studied in the present work. When the Cu is placed in one In(1) position (denoted as Cu1′ in Fig. 1), which is the third and the fourth NN to Fe1 and Fe2, respectively, corresponding to *b*-IFCO-V_O-*ii* configuration, it is found that the strong AFM coupling between Cu and Fe is varnished due to the absence of the O_{br} atoms between Cu and Fe. Figure 7 shows the projected DOSs (PDOSs) of Fe 3*d* and Cu 3*d* in FM ordering for *b*-IFCO-V_O-*ii* configuration. It is clear that the coupling between Fe 3*d* and Cu 3*d* states is very weak, which is attributed to the fact that the Cu atom is isolated from Fe pairs in this configuration. The weak coupling between Fe and Cu atoms is also evidenced by the spatial spin-density distribution (not shown here). In contrary, as seen in Figs. 5(f)–5(h), the Fe 3*d* and Cu 3*d* states as well as the 2*p* states of O_{br} are strong hybridized, which indicates a strong indirect FM coupling between Fe1 and Fe2 atoms. This also confirms the short-range effect of Cu doping. Moreover, when the Cu is positioned in the third and the first NN to Fe1 and Fe2, respectively, (*b*-IFCO-V_O-*iii*), there are two O_{br} atoms between Fe2 and Cu, but none between Fe1 and Cu. Strong AFM coupling exists between Fe2 and Cu while no coupling between Fe1 and Cu is found. As a consequence, the *b*-IFCO-V_O-*iii* system is a relatively weaker FM-coupled system (ΔE_{FM}=−45.6 meV) compared to *b*-IFCO-V_O-*i* configuration. These results, again, strongly support the importance of participation of codoped Cu in the hybridization of the Fe1:3*d*-O1:2*p*-Cu:3*d*-O2:2*p*-Fe2:3*d* orbital chain, which dominates the *e*-*e* correlations in IFCO-V_O system. Therefore, a long-range FM ordering needs large TM dopants concentration to form the continuous Fe1-O1-Cu-O2-Fe2 paths under the existence of V_O. This interpretation is tally with the previous findings that Fe- and Cu-codoped $In_2O_{3-\delta}$ show RT ferromagnetism with the Fe doping concentration larger than 10%.[14]

From the energy point of view, *b*-IFCO-V_O-*ii* is favored over *b*-IFCO-V_O-*i* by 0.08 eV. This, however, can be easily conquered in conventional sample preparation process. For example, at T=1000 °C, which is the common temperature for sample synthesis, the difference in stability, $\Delta E \sim 0.08$ eV, between *b*-IFCO-V_O-*ii* and *b*-IFCO-V_O-*i* configurations corresponds to a relative probability of the presence of *b*-IFCO-V_O-*i* being as high as 48%. On the other hand, although the *b*-IFCO-V_O-*ii* is energetically stable, its

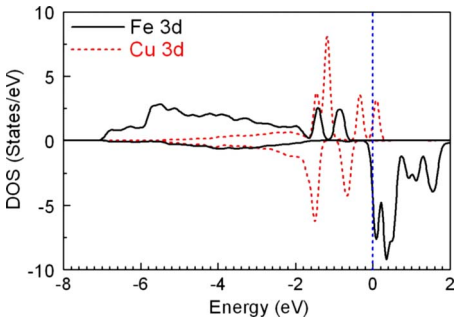

FIG. 7. (Color online) PDOSs of Fe 3*d* (black solid) and Cu 3*d* (red dashed) for *b*-IFCO-V_O-*ii* configurations in FM ordering. The vertical line drawn indicates the E_F position. The spin-up and spin-down DOSs are shown above and below the abscissa axis.

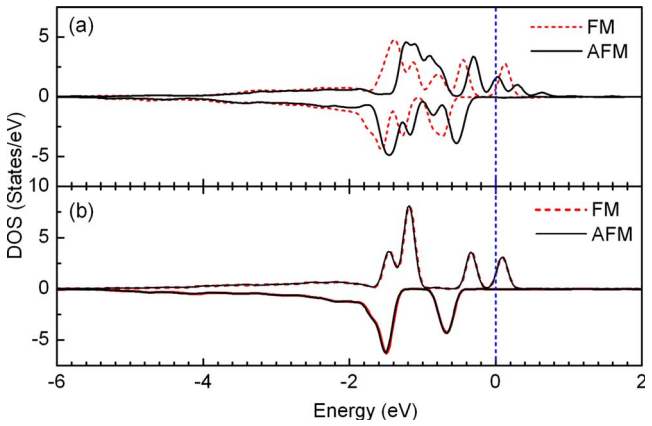

FIG. 8. (Color online) The Cu 3*d* PDOSs for (a) *b*-IFCO-V_O-*i* and (b) *b*-IFCO-V_O-*ii* configurations in both FM (red dashed) and AFM (black solid) orderings. The vertical line drawn indicates the E_F position. The spin-up and spin-down DOSs are shown above and below the abscissa axis.

ΔE_{FM} is only 7.1 meV as shown in Table II. Therefore, at RT, the AFM ordering in *b*-IFCO-V_O-*ii* configuration will be easily broken by the thermal energy, which makes the contribution of the ferromagnetic *b*-IFCO-V_O-*i* configuration dominated in the sample.

Figure 8 shows the PDOS of Cu 3*d* states of *b*-IFCO-V_O-*i* and *b*-IFCO-V_O-*ii* both in FM and AFM orderings. It is found that, for *b*-IFCO-V_O-*i* configuration, the strong coupling between Cu and Fe mediated by O_{br} causes a downward shifting of the Cu *d* bands to the valence band, resulting in more delocalized Cu *d* states in FM ordering compared to AFM ordering, which render the system FM ground state. On the other hand, in case of *b*-IFCO-V_O-*ii* configuration where the AFM is a more stable state, the splitting of Cu *d* orbital is almost identical for FM and AFM orderings. The identical splitting of Cu *d* orbital is also consistent with the isolated feature of the Cu atom in this configuration (*b*-IFCO-V_O-*ii*).

Further considerations have also been made on varying the position of V_O. Take *b*-IFCO-*i* for example. We investigated three configurations that the V_O is at the first NN to Fe but far away from Cu, and at the first NN to Cu but far away from Fe pairs, as well as the position out of the range of the second NN to both Cu and Fe. Regardless of V_O positions, FM prevails with ΔE_{FM} of −90.4, −29.3, and −41.8 meV, respectively. Similar results were obtained for *c*-IFCO-*i* system. Our calculations demonstrate a long-range effect of V_O on the ferromagnetism in IFCO system. The long-range effect of V_O is also evidenced in our previous experimental results[30] that the FM coupling can be switched on even with low carrier concentration of 10^{18} *e* cm^{-3}. Further experimental supports can be found from the work of Yu *et al.*,[10] where they found that the FM coupling in IFCO-V_O system is mediated by delocalized carriers.

There are two possible mechanisms proposed for FM semiconductor: carrier mediated and superexchange. The key difference between these two mechanisms is that the magnetic coupling is mediated by mobile carriers in the former but by localized anions in the latter. In our case, the AFM superexchange interaction between Fe and Cu atoms follows a path through the intermediate O anion which results in an indirect FM coupling between Fe atoms. The main mechanism is the hybridization of the Fe *d* states with the O *p* and subsequently with the Cu *d* states. In the structures with pronounced ferromagnetism, the hybridization of the Cu *d* states with the O *p* is particularly enhanced. That effect is assisted by the downward shift of the Cu $3d_{xy}$ and $3d_{yz}$ spin majority band which overlaps (in energy scale) more with the O *p* band. This mechanism was more evident for the structures *b*-IFCO-V_O-*i* and *c*-IFCO-V_O-*i*, which are found to have strong FM ground states. The *p*-*d* hybridization induces a remote electron delocalization which mediates the Fe-Fe interaction. On the contrary, the long-range carrier-mediated mechanism is switched on by delocalized electrons introduced by V_O, which mediate the different Fe1-O1-Cu-O2-Fe2 chains.

IV. CONCLUSIONS

In summary, we systematically studied the effect of Cu codoping and V_O on the ferromagnetism in Fe-doped In_2O_3 by detailed first-principles calculations. It has been demonstrated that IFOs are in AFM ground state for all configurations investigated. With the existence of V_O, IFO can be weakly FM ground state when the O_{br} between Fe1 and Fe2 is leaking, which acts to mediate the superexchange interaction leading to AFM coupling between Fe1 and Fe2. By additional Cu doping, strong ferromagnetism appears in the IFCO-V_O system. Examination of spin-density distribution and DOS spectra reveals that the couplings between Cu and Fe are AFM for both Fe1 and Fe2 mediated by the O_{br} atoms. Thus, the strong indirect FM interaction among Fe cations is formed via the Fe1-O1-Cu-O2-Fe2 coupling chains. The role of the Cu^{2+} ions in IFCO is to act as superexchange mediators by causing an indirect FM coupling between Fe cations through the hybridization of the O 2*p* states with 3*d* states of Cu and Fe, thereby enhancing the ferromagnetism.

Our calculations suggest that the ferromagnetism in IFCO system can be achieved with a large doping concentration of Fe with coexistence of V_O. The large Fe doping concentrations would result in an average smaller Fe-Cu separation distance, which increases the chance to form the Fe1-O1-Cu-O2-Fe2 coupling chains. The concentration of V_O, however, is not critical due to its long-range coupling effect.

ACKNOWLEDGMENTS

This work was in part supported by Nanyang Technological University and Ministry of Education of Singapore under Grants No. RG34/05, No. RG57/05, No. RG59/06, and No. T207B1217) and by Singapore A*star SERC under Grant No. 062 101 0030.

*jlkuo@ntu.edu.sg
†wanglan@ntu.edu.sg

[1] T. Dietl, H. Ohno, F. Matsukura, J. Cibert, and D. Ferrand, Science **287**, 1019 (2000).
[2] J. M. D. Coey, M. Venkatesan, and C. B. Fitzgerald, Nature Mater. **4**, 173 (2005).
[3] A. Gupta, H. Cao, K. Parekh, K. V. Rao, A. R. Raju, and U. V. Waghmare, J. Appl. Phys. **101**, 09N513 (2007).
[4] S.-J. Hu, S.-S. Yan, X.-L. Lin, X.-X. Yao, Y.-X. Chen, G.-L. Liu, and L.-M. Mei, Appl. Phys. Lett. **91**, 262514 (2007).
[5] C. B. Fitzgerald, M. Venkatesan, A. P. Douvalis, S. Huber, J. M. D. Coey, and T. Bakas, J. Appl. Phys. **95**, 7390 (2004).
[6] J. R. Neal, A. J. Behan, R. M. Ibrahim, H. J. Blythe, M. Ziese, A. M. Fox, and G. A. Gehring, Phys. Rev. Lett. **96**, 197208 (2006).
[7] S. B. Ogale, R. J. Choudhary, J. P. Buban, S. E. Lofland, S. R. Shinde, S. N. Kale, V. N. Kulkarni, J. Higgins, C. Lanci, J. R. Simpson, N. D. Browning, S. Das Sarma, H. D. Drew, R. L. Greene, and T. Venkatesan, Phys. Rev. Lett. **91**, 077205 (2003).
[8] M. H. F. Sluiter, Y. Kawazoe, P. Sharma, A. Inoue, A. R. Raju, C. Rout, and U. V. Waghmare, Phys. Rev. Lett. **94**, 187204 (2005).
[9] J. Philip, A. Punnoose, B. I. Kim, K. M. Reddy, S. Layne, J. O. Holmes, B. Satpati, P. R. LeClair, T. S. Santos, and J. S. Moodera, Nature Mater. **5**, 298 (2006).
[10] Z. G. Yu, J. He, S. Xu, Q. Xue, O. M. J. van't Erve, B. T. Jonker, M. A. Marcus, Y. K. Yoo, S. Cheng, and X. D. Xiang, Phys. Rev. B **74**, 165321 (2006).
[11] H. Raebiger, S. Lany, and A. Zunger, Phys. Rev. Lett. **101**, 027203 (2008).
[12] S. J. Pearton, C. R. Abernathy, M. E. Overberg, G. T. Thaler, D. P. Norton, N. Theodoropoulou, A. F. Hebard, Y. D. Park, F. Ren, J. Kim, and L. A. Boatner, J. Appl. Phys. **93**, 1 (2003).
[13] K. L. Chopra, S. Major, and D. K. Pandya, Thin Solid Films **102**, 1 (1983).
[14] J. He, S. Xu, Y. K. Yoo, Q. Xue, H.-C. Lee, S. Cheng, X. D. Xiang, G. F. Dionne, and I. Takeuchi, Appl. Phys. Lett. **86**, 052503 (2005).
[15] Y. K. Yoo, Q. Xue, H.-C. Lee, S. Cheng, X. D. Xiang, G. F. Dionne, S. Xu, J. He, Y. S. Chu, S. D. Preite, S. E. Lofland, and I. Takeuchi, Appl. Phys. Lett. **86**, 042506 (2005).
[16] M. J. Reed, F. E. Arkun, E. A. Berkman, N. A. Elmasry, J. Zavada, M. O. Luen, M. L. Reed, and S. M. Bedair, Appl. Phys. Lett. **86**, 102504 (2005).
[17] K. R. Kittilstved, N. S. Norberg, and D. R. Gamelin, Phys. Rev. Lett. **94**, 147209 (2005).
[18] S. Kuroda, N. Nishizawa, K. Takita, M. Mitome, Y. Bando, K. Osuch, and T. Dietl, Nature Mater. **6**, 440 (2007).
[19] T. Dietl, Nature Mater. **5**, 673 (2006).
[20] N. N. Lathiotakis, A. N. Andriotis, and M. Menon, Phys. Rev. B **78**, 193311 (2008).
[21] P. Kharel, C. Sudakar, M. B. Sahana, G. Lawes, R. Suryanarayanan, R. Naik, and V. M. Naik, J. Appl. Phys. **101**, 09H117 (2007).
[22] N. H. Hong, J. Sakai, N. T. Huong, and V. Briz, J. Magn. Magn. Mater. **302**, 228 (2006).
[23] N. H. Hong, J. Sakai, N. T. Huong, and V. Brize, Appl. Phys. Lett. **87**, 102505 (2005).
[24] G. Peleckis, X. Wang, and S. X. Dou, Appl. Phys. Lett. **89**, 022501 (2006).
[25] G. Peleckis, X. L. Wang, and S. X. Dou, IEEE Trans. Magn. **42**, 2703 (2006).
[26] M. Sasaki, K. Yasui, S. Kohiki, H. Deguchi, S. Matsushima, M. Oku, and T. Shishido, J. Alloys Compd. **334**, 205 (2002).
[27] S. Kohiki, M. Sasaki, Y. Murakawa, K. Hori, K. Okada, H. Shimooka, T. Tajiri, H. Deguchi, S. Matsushima, M. Oku, T. Shishido, M. Arai, M. Mitome, and Y. Bando, Thin Solid Films **505**, 122 (2006).
[28] L. A. Errico, M. Rentería, and M. Weissmann, Phys. Rev. B **72**, 184425 (2005).
[29] C. E. Rodriguez-Torres, A. F. Cabrera, L. A. Errico, C. Adan, F. G. Requejo, M. Weissmann, and S. J. Stewart, J. Phys.: Condens. Matter **20**, 135210 (2008).
[30] H. W. Ho, B. C. Zhao, B. Xia, S. L. Huang, J. G. Tao, A. C. H. Huan, and L. Wang, J. Phys.: Condens. Matter **20**, 475204 (2008).
[31] D. Chu, Y.-P. Zeng, and D. Jiang, Appl. Phys. Lett. **92**, 182507 (2008).
[32] P. E. Blöchl, Phys. Rev. B **50**, 17953 (1994).
[33] G. Kresse and J. Furthmuller, Comput. Mater. Sci. **6**, 15 (1996).
[34] G. Kresse and J. Furthmüller, Phys. Rev. B **54**, 11169 (1996).
[35] G. Kresse and D. Joubert, Phys. Rev. B **59**, 1758 (1999).
[36] J. P. Perdew, K. Burke, and M. Ernzerhof, Phys. Rev. Lett. **77**, 3865 (1996).
[37] J. E. Medvedeva, Phys. Rev. Lett. **97**, 086401 (2006).
[38] L.-H. Ye, A. J. Freeman, and B. Delley, Phys. Rev. B **73**, 033203 (2006).